A novel non-flammable electrolyte containing methyl nonafluorobutyl ether for lithium secondary batteries

J. ARAI

Hitachi Research Laboratory, Hitachi Ltd, 1-1, Omika-cho 7-chome, Hitachi-shi, Ibaraki-ken 319-1292, Japan
(fax: +81 294 52 7636, e-mail: jarai@hrl.hitachi.co.jp)

Abstract

Use of nonflammable fluorinated ethers as electrolytes for lithium secondary batteries has been studied in terms of the flammability, ionic conductivity and cell charge–discharge performances including the rate capability, cycle life and abuse (nailing) test of a graphite/$LiCoO_2$ cylindrical cell. By mixing appropriate amounts of methyl nonafluorobutyl ether (MFE) with cosolvents (e.g., ethyl methyl carbonate (EMC) and diethyl carbonate (DEC)), the mixed solution showed no flash point when evaluated by the Cleaveland open-cup flash point method (JIS 2265). The ionic conductivity was investigated for various electrolytes containing MFE with some lithium salts including $LiN[SO_2C_2F_5]_2$ (LiBETI) and $LiN[SO_2CF_3]_2$ (LiTFSI). The solution properties of the electrolytes containing MFE were characterized in terms of the NMR chemical shifts and the diffusion coefficients by using the NMR pulse field gradient method. The graphite/$LiCoO_2$ cylindrical cells assembled with 1 mol dm^{-3} LiBETI–MFE/EMC (80:20 vol %) discharged the designed capacity (1400 mAh) at a 0.1 C rate and sustained 80% of their initial capacity up to 50 cycles. No thermal runaway was detected and cell surface temperature increased very slowly in the nailing test which meant hardly any software and hardware protections were necessary.
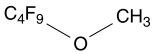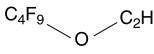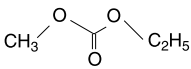
1. Introduction

Lithium secondary batteries possess two to three times higher energy density than other secondary batteries using aqueous electrolytes which has made them the state-of-the-art battery in portable electronic products such as cellular phones, laptop computers and camcorders [1]. Their high operation voltage (over 3 V) requires a nonaqueous electrolyte because this voltage is above the oxidation voltage of water. Nonaqueous electrolytes present a safety concern because they contain flammable organic solvents having a low flash point (f.p.): for example, dimethyl carbonate (DMC; f.p. 17 °C), ethyl methyl carbonate (EMC; f.p. 23 °C), diethyl carbonate (DEC; f.p. 33 °C) and dimethoxy ethane (DME; f.p. 0 °C) [1–5]. Though commercial batteries are firmly based in safety devices such as a current intermitted device (CID) and a positive temperature coefficient (PTC) device [6], an inherently safe battery is desired which uses a nonflammable electrolyte.

Challenges to the development of nonflammable electrolytes have been made recently using mixed fire-retardant additives [6–8] and halogenated solvents [9, 10]. A few weight percent of hexamethoxycyclotriphosphazene $[-N{=}P(OCH_3)_2-]_3$ depressed the heat generation of the electrolyte (1 mol dm^{-3} $LiPF_6$–EC/DMC)

at elevated temperature in ARC (accelerating rate calorimeter) measurements [6]. By addition of trimethylphosphate (TMP), the burn velocities of electrolytes were depressed in the horizontal burning test based on UL94 [7]. The addition of a high content of TMP was found to affect charge–discharge capacities of the carbonaceous anode [8]. Although these electrolytes still contain low f.p. solvents as their main component, halogen atoms are expected to quench radical species in the burning reaction and depress the combustion. We have studied an electrolyte containing trifluoropropylene carbonate (TFPC) [9]. Furthermore, we found an electrolyte composed of TFPC and chloroethylene carbonate (ClEC) had a high f.p. of more than 100 °C and showed good cell performance in graphite/Li and $Li_{1+x}Mn_2O_4$/Li cells [10]. However, these electrolytes still have flash points. Our new approach for intrinsic safety of lithium secondary batteries is use of nonflammable solvents having no flash points as the electrolytes.

Fluorinated solvents are suitable candidates for this purpose because we can choose the desired chemical and physical properties to design the electrolytes. Though perfluoroalkanes and semifluoroalkanes having twice as many fluorine atoms as hydrogen atoms are usually nonflammable, these compounds do not easily dissolve lithium salts and they do not mix readily with ordinary

Table 1. Chemical structures and relevant properties of alkyl-fluoroalkyl ethers (AFE) and ethyl methyl carbonate

Solvent	Methyl nonafluorobutyl ether (MFE)	Ethyl nonafluorobutyl ether (EFE)	Ethyl methyl carbonate (EMC)
Chemical structure	C_4F_9—O—CH_3	C_4F_9—O—C_2H_5	CH_3—O—C(=O)—O—C_2H_5
Molecular weight	250	264	104
Melting point/°C	−135	−117	−55
Boiling point/°C	60	73	107
Flash point/°C	no f.p.	no f.p.	23
Viscosity/10^7 m^2 s^{-1}	3.8	3.8	7.0
Surface tension/10^3 N m^{-1}	14	14	27
Density/kg dm^{-3}	1.52	1.43	1.01

electrolyte solvents like carbonates, ethers and esters. The introduction of functional groups having oxygen atoms such as carbonyl (ketone) or carboxyl (esters) groups to overcome these two problems of fluorinated compounds results in flammable compounds. Thus, we chose alkyl fluoroalkyl ethers (AFE) as nonflammable solvents; they have a minimum number of oxygen atoms and are expected to mix readily with conventional electrolyte solvents. We focused on methyl nonafluorobutyl ether (MFE) and ethyl nonafluorobutyl ether (EFE) because these solvents have low molecular weights and an appropriate liquid phase temperature range. These solvents have advantages of low viscosities and surface tensions compared to conventional solvents (e.g., EMC) as listed in Table 1.

This work presents physical and electrochemical properties of mixed solvent electrolytes containing nonflammable AFE (i.e., MFE and EFE), including properties of conductivity, flash points, chemical shifts, diffusion coefficients, charge–discharge capacities, rate performance, and cycle life. Results from the nailing test as an abuse test are also described.

2. Experimental details

2.1. *Electrolyte preparation*

The electrolytes were prepared by mixing nonflammable solvent (i.e., MFE or EFE purchased from 3M Company) with conventional electrolyte solvents as cosolvent by volume percent. We investigated EMC, DMC, DEC, DME, diethylene glycol dimethyl ether (DGM), triethylene glycol dimethyl ether (TGM), ethylene carbonate (EC), propylene carbonate (PC), butylene carbonate (BC), 1,3-dioxolane (DOL) and γ-butyrolacton (GBL) as cosolvents. All these cosolvents were obtained from Tomiyama Yakuhin Kogyo as battery grade solvents containing less than 20 ppm of water. Necessary amounts of lithium salts were then dissolved into the mixed solvents to make the electrolyte solution of the designated concentration (M; mol dm^{-3}). The lithium

salts investigated in this study were $LiBF_4$ and $LiPF_6$ both from Tomiyama Yakuhin Kogyo, $LiN(SO_2CF_3)_2$ (lithium bis[trifluoromethylsulfonyl] imide: LiTFSI), $LiN(SO_2C_2F_5)_2$ (lithium bis[pentafluoroethylsulfonyl] imide: LiBETI) from 3M Company and $LiN(SO_2 C_4F_9)(SO_2CF_3)$ (lithium nonafluorobutylsulfonyl trifluoromethylsulfonyl imide: LiFBMSI) from Central Glass Company.

We prepared the electrolytes and stored them in bottles in an argon filled glove box kept at less than −80 °C of the dew point of water. The LiTFSI, LiBETI and LiFBMSI were vacuum dried for more than 24 h at 120 °C prior to use.

2.2. *Flash point, conductivity and NMR measurements*

The flash points of the mixed solvents were evaluated by the Cleaveland open-cup flash point method based on JIS 2265 (Japanese Industrial Standard), or ASTM D-92 (American Society for Testing and Materials). These standards are testing methods of flash point for petroleum products such as gasoline, diesel oil, kerosene, lubricants *etc.* The flash point test detects the temperature when the liquid flames. The flash points were determined as an average of three consecutive tests.

The conductivity of each electrolyte was measured with a Toa CM–30V conductivity meter at a frequency of 3 kHz and 25 °C in a cell with parallel Pt electrodes.

The solvation strength of each solvent in the electrolyte was evaluated by the solvation shift [9–11] defined in Equation 1:

$$\Delta\delta = \delta_{\text{electrolyte}} - \delta_{\text{solvent}} \qquad (1)$$

($\delta_{\text{electrolyte}}$: chemical shift of the solvent in electrolyte solution with lithium salt, δ_{solvent}: chemical shift of the solvent in solution without lithium salt.) ^{13}C-NMR chemical shifts of each solvent in the solution were measured by a Jeol JNM-400GX FT-NMR spectrometer with an external standard of tetramethylsilane and proton decoupling mode, locked with the signal of $CDCl_3$.
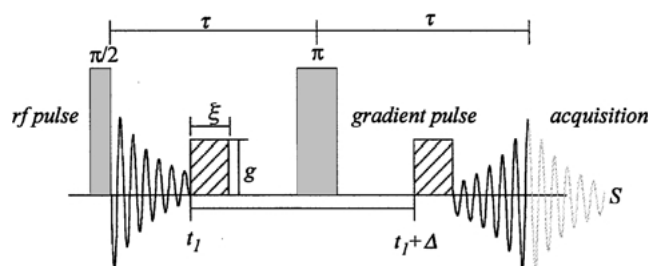
Fig. 1. A schematic representation of the PFG-NMR pulse sequence for measuring diffusion coefficients.

Diffusion coefficients of ^{1}H for solvents, and [7]Li and ^{19}F for lithium salts of selected electrolytes were evaluated by a pulse field gradient (PFG) NMR method [13–15]. The PFG-NMR spectra of ^{1}H, [7]Li and ^{19}F were measured using a Varian Unity Plus 500 spectrometer with a pulse sequence as illustrated in Figure 1. When the magnetic pulse field with a magnitude g is applied, the NMR signal $S\langle g\rangle$ is attenuated. The attenuation of the PFG-NMR signal is related to the experimental parameters (i.e., ξ, g and Δ) and the diffusion coefficient D of the observed molecule by Equation 2 [16]:

$$\ln\left(\frac{S\langle g\rangle}{S\langle g=0\rangle}\right) = -D\left[\gamma^2\xi^2 g^2\left(\Delta - \frac{\xi}{3}\right)\right] \qquad (2)$$

($S\langle g=0\rangle$ is the NMR signal without the pulse field, $S\langle g\rangle$ is the NMR signal with the pulse field, γ is the magnetogyric ratio of the observed nucleus, g is the pulse magnitude, ξ is the pulse duration, D is the diffusion coefficient of the molecule related to the observed nucleus.) We could estimate D by the slope from the plot of $\ln(S\langle g\rangle/S\langle g=0\rangle)$ against $\gamma^2\xi^2 g^2(\Delta - \xi/3)$. The γ for ^{1}H, [7]Li and ^{19}F nuclei are 267.51, 103.96 and 251.665 M rad T^{-1} s^{-1}, respectively. The Δ values used were 20, 50 and 100 ms. The ξ used was 4 ms.

2.3. Evaluation of charge–discharge performances in a graphite/LiCoO$_2$ cylindrical cell

Graphite/LiCoO$_2$ 18 650 type cylindrical cells (18 mm dia. × 65 mm high) were assembled with the selected nonflammable electrolyte (1 M LiBETI–MFE/EMC (80:20)) and 1 M LiPF$_6$–EC/EMC (30:70) for comparison. The anode was produced by coating and drying a paste composed of synthetic graphite (90 wt %) and polyvinylidenefluoride (PVDF) binder (10 wt %) on copper foil. The cathode was prepared by coating and drying a paste made of LiCoO$_2$ (85 wt %), a graphite conducting supporter (8 wt %) and PVDF binder (7 wt %) on aluminum foil. The CID and PTC were located inside the cell.

The charge–discharge operation of the cell was controlled by a Toscat 3000 battery tester (Toyo System). The cells were charged with a constant current to 4.1 V and then with a constant voltage of 4.1 V until the current reached 10 mA or 15 h had passed. The cells were discharged with a constant current by a cut-off voltage of 2.8 V. The nailing test was carried out with specially designed equipment consisting of a cell holder and an oil press cylinder which held a nail (5 mm dia.).

3. Results and discussion

3.1. Solubility of the cosolvents in MFE

We first investigated the solubility of the cosolvents in MFE, because MFE and EFE alone do not dissolve the lithium salts examined in this study. A 20 vol % of cosolvent was mixed with 80 vol % of MFE. The results are listed in Table 2. All cosolvents having a linear chemical structure (DMC, EMC, DEC, DME, DGM, TGM) and DOL were well dissolved in MFE and gave clear mixed solutions. The mixed solutions of EC, PC

Table 2. Solubility in MFE and calculated dipole moment of cosolvents

Cosolvent	Dimethoxy ethane (DME)	Diethylene glycol dimethyl ether (DGM)	Triethylene glycol dimethyl ether (TGM)	Dimethyl carbonate (DMC)	Ethyl methyl carbonate (EMC)
Chemical structure					
Solubility	good	good	good	good	good
Dipole moment/Debye	0.00	1.39	0.00	0.76	0.89
Cosolvent	Diethyl carbonate (DEC)	1,3-Dioxolane (DOL)	γ-Butyrolacton (GBL)	Ethylene carbonate (PC)	Propylene carbonate (PC)	Butylene carbonate (BC)
Chemical structure						
Solubility	good	good	separated	separated	separated	separated
Dipole moment/Debye	0.97	1.26	4.23	4.62	4.81	5.01

and BC with MFE each separated into two phases. The solubility of cosolvent in MFE did not depend on the functional group or the chemical structure. The dipole moments derived from molecular orbital (MO) calculations (using the *ab initio* MO program of Gaussian 94 W with the 6-31G** basis set including the polarization functions) of all cosolvent molecules examined in this experiment are also listed in Table 2. The calculated dipole moment of MFE was 2.37 Debye. Cosolvents possessing lower dipole moments than that of MFE mixed well with it. The electrostatic interaction between MFE and cosolvent may be the dominant factor which controls the homogeneity of the mixture. We thought that cosolvent molecules having high dipole moments would aggregate with each other and be unaffected by the electrostatic interaction of AFE. Consequently, we chose low dipole moment cosolvents to mix with AFE for the nonflammable electrolytes.

3.2. Flash points of MFE and EFE mixed solvents

We examined flash points of the mixed solvents containing AFE by the Cleaveland open-cup flash point method. EMC was selected as a representative cosolvent to analyse the behaviour of flash points as the mixing amount of AFE was changed. Mixed solvents containing 0, 20, 40, 60 and 80 vol % of MFE and EFE were prepared and results of their flash point tests are listed in Table 3. The flash point increased as the MFE amounts increased and for the mixing ratio of 80 vol % there was no flame. The flash points of the EFE/EMC mixed solvents, however, decreased with increasing EFE amounts. Since combustion takes place in the gas phase, the evaporation of the mixed solvents should be considered to investigate the behaviour of their flash points. When, mixed solvent is heated, the solvent evaporates independently from each component at certain temperatures. The flash point may depend upon the evaporation rate of combustible species (i.e., EMC in this case), and the ratio of the EMC and MFE (nonflammable species) and oxygen. We thought that the evaporation rate of EMC in MFE/EMC mixed solution was smaller than in pure solvent and an MFE-rich vapour was formed which led to higher flash points than that of pure EMC for MFE/EMC mixed solvents throughout the MFE volume ratio. Conversely, more

EMC might evaporate in the EFE/EMC mixed solvents than in the pure EMC solvent leading to lower flash points, because the evaporation depended upon the interaction force between solvent molecules making up the solution.

The flash point of the AFE mixed solvent depends on the combination of components which influences interaction between the solvent molecules. Thus, the flammability of the mixed solvent solution should be examined case by case because it is difficult to predict interaction between the solvent molecules. Molecular features of AFE related to the flame retardant ability are another factor which affects the flammability. In general, this fire retardant ability of fluorinated compounds depends on the ratio of fluorine atoms to hydrogen atoms (F/H ratio) in the chemical structure. Based on the F/H ratio, it was clear that MFE had higher fire retarding ability than EFE. Accordingly, we chose MFE as solvent for the nonflammable electrolyte and examined flash points of mixed solvents with other cosolvents.

We prepared mixed solvents containing 70, 80 and 90 vol % of MFE with cosolvents of DME, DMC, EMC, DEC and TGM and measured their flash points. MFE/DGM and MFE/DOL were excluded because their solutions were cloudy or partially separated when lithium salt was added. Table 4 summarizes the flash point test results. The flash point of the mixed solutions showed a dependency on the flash point of pure cosolvent. Thus, a high flash point cosolvent needed a smaller amount of MFE than a low flash point one to obtain a nonflammable mixed solvent solution. We obtained nonflammable solutions with more than 70 vol % MFE in MFE/DEC and MFE/TGM, and more than 80 vol % MFE in MFE/EMC and MFE/DMC, and 90 vol % MFE in MFE/DME.

3.3. Conductivities of the electrolytes containing MFE

We chose EMC as a representative cosolvent with MFE and investigated the solubility of lithium salt in MFE/EMC and also measured conductivity for the electrolyte containing MFE. Figure 2 shows the conductivity of MFE/EMC (80:20) mixed solution as a function of the lithium salt concentration for $LiBF_4$, $LiPF_6$, LiTFSI, LiBETI and LiFBMSI. Less than 0.2 M $LiBF_4$ and $LiPF_6$ were dissolved in MFE/EMC (80:20) solution. With more than 0.3 M $LiBF_4$ or $LiPF_6$, the solution

Table 3. Flash points of AFE and EMC mixed solvents

Volume fraction of AFE/vol %	Flash point/°C	
	Methyl nonafluorobutyl ether (MFE)	Ethyl nonafluorobutyl ether (EFE)
0	23.0	23.0
20	24.3	21.5
40	28.8	19.5
60	34.5	15.5
80	no f.p.	13.0

Table 4. Flash points of MFE and cosolvent solutions

Volume fraction of MFE/vol %	Flash point/°C				
	DME	DMC	EMC	DEC	TGM
0	0	17	23	33	113
70	8	41	58	no f.p.	no f.p.
80	38	no f.p.	no f.p.	no f.p.	no f.p.
90	no f.p.	no f.p.	no f.p.	no f.p.	no f.p.

Fig. 2. Conductivity of MFE/EMC (80:20) with various lithium salts as a function of salt concentration.

Fig. 3. Conductivity of LiTFSI–MFE/linear carbonate (80:20) as a function of salt concentration.
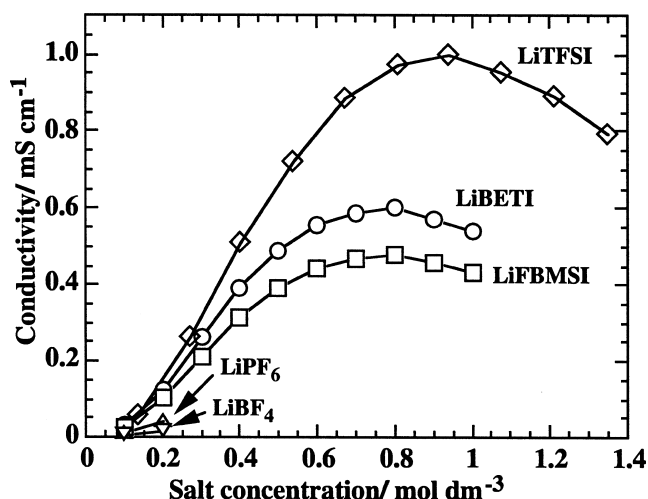

Fig. 4. Conductivity of LiTFSI–MFE/EMC (80:20) and MFE/TGM (80:20) as a function of salt concentration.

separated into two phases. The maximum conductivities of LiBF$_4$–MFE/EMC and LiPF$_6$–MFE/EMC were 0.015 mS cm^{-1} and 0.042 mS cm^{-1}, respectively. More than 1 M LiTFSI, LiBETI and LiFBMSI dissolved in MFE/EMC solution. The LiTFSI–MFE/EMC electrolyte showed a maximum conductivity of 0.97 mS cm^{-1} at 0.94 M. LiBETI–MFE/EMC and LiFBMSI–MFE/EMC showed maximum conductivities of 0.6 mS cm^{-1} and 0.48 mS cm^{-1} both at around 0.8 M, respectively. Because MFE does not have a strong ability to solvate ions (Li$^+$ and anions) compared to EMC, EMC may coordinate to the ions more than MFE does. PF$_6^-$ and BF$_4^-$ have a spherical charge distribution and they are smaller than organic anions. This feature of inorganic anions may affect the interaction between EMC and MFE and induce phase separation in the mixed solution with inorganic lithium salts. Organic anions may have a broad charge distribution due to their size and possible conjugation structures [17, 18] which prevents the phase separation.

In the case of DMC and DEC with LiTFSI, we saw the same conductivity behaviour with salt concentration for MFE/DMC (80:20) and MFE/DEC (80:20) solutions as shown in Figure 3. MFE/DMC solution had a maximum conductivity of 0.84 mS cm^{-1} at 1.0 M and MFE/DEC had a maximum conductivity of 0.69 mS cm^{-1} at 0.9 M. MFE/EMC (80:20) showed the highest conductivity of these solutions. The number of molecules presented in the same volume mixture follows the order DMC > EMC > DEC, because the densities of these solvents are almost the same. However, the solvation enthalpies of these solvents are in the order of DEC > EMC > DMC [9, 12]. The balance of solvation enthalpy and the number of solvent molecules was one possible factor which led to the MFE/EMC electrolyte having the highest conductivity among these electrolytes.

LiTFSI–MFE/ether (80:20) electrolytes showed higher conductivities than LiTFSI–MFE/carbonate electrolytes (Figure 4). The maximum conductivities of MFE/DME and MFE/TGM were 1.30 mS cm^{-1} and
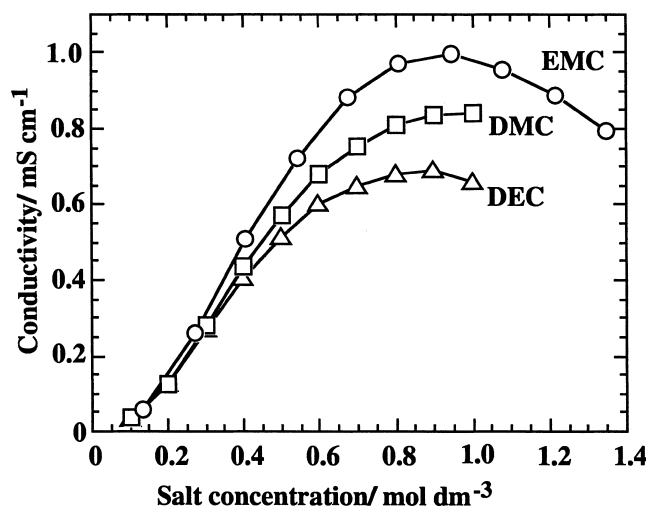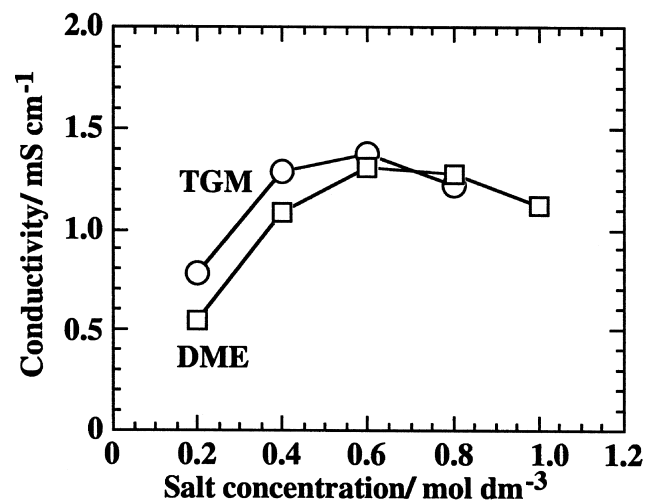
1.38 mS cm^{-1} both at 0.6 M, respectively. Considering that the solvation enthalpies of the ether molecules are smaller than those of the carbonate molecules [19, 20], the association constant of lithium salt in MFE/ether electrolytes must be larger than in MFE/carbonate electrolytes. This should lead to smaller conductivity in MFE/ether electrolytes than in MFE/carbonate electrolytes. The results, however, were the opposite to this. This may be due to the difference between solvation structure of Li$^+$-carbonate solvents and Li$^+$-ether solvents which are known to use bidented coordination leading to a smaller solvation structure than for carbonate solvents [21].

3.4. Solvation shifts and diffusion coefficients of the electrolytes containing MFE

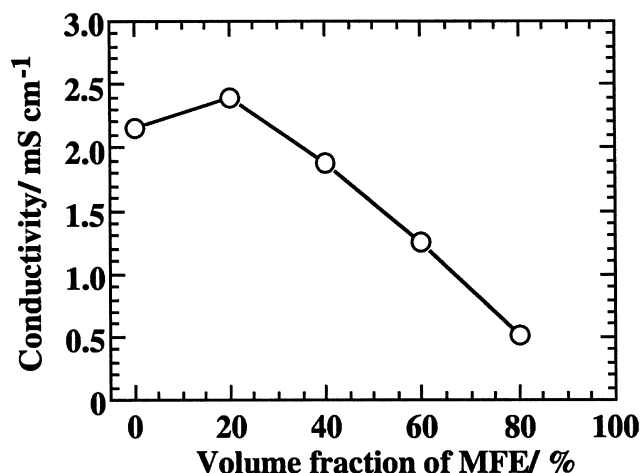Figure 5 shows the conductivity of 1 M LiBETI–MFE/EMC electrolyte as a function of MFE volume ratio.

Fig. 5. Conductivity of 1 M LiBETI–MFE/EMC as a function of MFE volume fraction.

The conductivity of the electrolyte initially increased with addition of small amounts of MFE and at 20 vol %, there was a maximum conductivity of 2.39 mS cm^{-1}. At this mixing ratio, the molecular ratio of Li ion:MFE:EMC was about 1:8:1. Considering the solvation number of ions for an EMC molecule is 4 [12, 22–24], all the EMC molecules are involved in solvation at this MFE mixing ratio and the EMC solvated ions are surrounded by free MFE. In the case of 1 M LiBETI–EMC electrolyte (pure EMC system), the EMC solvated ions are surrounded by free EMC. The low viscosity of MFE may allow faster movement of the EMC solvated ions in the MFE/EMC electrolyte at 20 vol % of MFE mixing ratio than in the pure EMC electrolyte.

The solvation shifts $\Delta\delta$ of EMC and MFE were evaluated by measuring ^{13}C-NMR chemical shift in 1 M LiBETI–MFE/EMC electrolytes as a way to investigate the solvent-ion interaction. The solvation shift $\Delta\delta$ is induced by the electron density change of the observed nucleus [10, 25] due to solvation of the ions. MO calculations have suggested that the solvation shift $\Delta\delta$ of solvent molecules is mainly due to coordination of solvent to Li$^+$ ions [11]. Figure 6 shows the change of the solvation shift $\Delta\delta$ of EMC and MFE in 1 M

LiBETI–MFE/EMC electrolytes as a function of MFE volume ratio. The atom positions for all evaluated $\Delta\delta$ are indicated on the chemical structure for each solvent. A positive shift indicates the low magnetic field and a decrease of electron density around the observed nucleus. The $\delta_{\text{electrolyte}}$ is expressed by a weighted average of solvated solvent molecules (solvent-Li$^+$ adduct) and free solvent molecules as presented in Equation 3:

$$\delta_{\text{electrolyte}} = \frac{\chi_{\text{adduct}} \times \delta'_{\text{adduct}} + \chi_{\text{free}} \times \delta'_{\text{free}}}{\chi_{\text{adduct}} + \chi_{\text{free}}} \tag{3}$$

(χ_{adduct}, χ_{free}, δ'_{adduct}, and δ'_{free} represent the number of solvated solvent molecules, the number of free solvent molecules, the critical chemical shift for solvated solvent molecules, and the critical chemical shift for single solvent molecules, respectively.) Thus, the solvation shift $\Delta\delta$ decreases with increase of free solvents. The solvation shift $\Delta\delta$(a) of OCH$_3$ carbon in MFE was observed in a low MFE volume ratio region of less than 40 vol %. This suggested that MFE solvated Li$^+$ in this region, though the solvation force may be small. There was a small solvation shift in the high MFE volume ratio region, indicating that MFE did not solvate enough Li$^+$ in this region where the $\Delta\delta$ of EMC was a maximum. The facts suggested that the ratio of solvated MFE in the total MFE molecules was very small. The solvation shifts $\Delta\delta$(b, c, e) of >C=O, OCH$_2$ and OCH$_3$ carbon in EMC were larger than $\Delta\delta$(a) in MFE, indicating that EMC solvated Li$^+$ much more strongly than the MFE did over the whole MFE volume ratio range. Thus, EMC may selectively solvate Li$^+$ in 1 M LiBETI–MFE/EMC electrolyte. The $\Delta\delta$(b, c, e) of EMC increased when MFE volume ratio was more than 60 vol %. At this volume ratio, the molar ratio of EMC/Li$^+$ (3.8:1) was less than 4. This meant that there must be an increase of ion-pair structure or increasing association of lithium salt. The solvation shift $\Delta\delta$(d) of CH$_3$ in EMC was negative (upper magnetic field shift meaning an increase of electron density) because of the charge alternation induced by solvation using >C=O oxygen binding [11], and –OCH$_2$ or –OCH$_3$ oxygen bonding, according to the MO calculations. We sug-
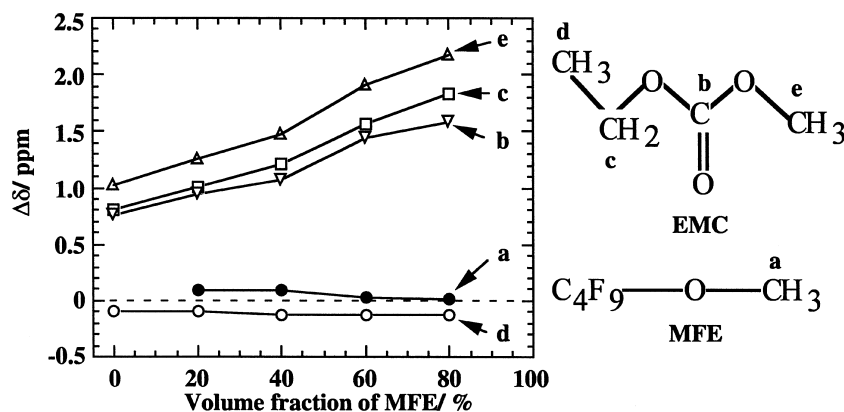

Fig. 6. Solvation shift $\Delta\delta$ of ^{13}C-NMR in 1 M LiBETI–MFE/DME as a function of MFE volume fraction.

Table 5. Diffusion coefficients, experimental conductivities (σ_{exp}) and association constants (K_a)

Electrolyte composition	Diffusion coefficient/10^{-10} m^2 s^{-1}					σ_{exp}/mS cm^{-1}	K_a
	MFE	EMC	BETI$^-$	PF$_6^-$	Li$^+$		
1 M LiBETI–MFE/EMC (80:20)	5.1	3.2	1.8		2.0	0.56	20.5
1 M LiBETI–EMC		6.5	2.8		2.4	2.1	7.3
1 M LiPF$_6$–EMC		5.6		2.9	2.8	4.0	5.4

gested that the coordination structure of EMC might not change much in MFE/EMC mixed solvent electrolyte.

We also investigated the diffusion coefficients of 1 M LiBETI–MFE/EMC (80:20) and two related electrolytes by the PFG-NMR method. The results are summarized in Table 5. The diffusion coefficient D is expressed by the Stokes–Einstein equation as presented in Equation 4:

$$D = \frac{K_b T}{C \pi \eta r_s} \quad (4)$$

where K_b denotes the Boltzmann constant, T denotes the absolute temperature, C is a constant and is usually 6, η is viscosity and r_s is an ion radius.

In the electrolyte, the solvent exists as a solvated state, an ion-pair state and a free state. Thus, the diffusion coefficient of solvent is also a weighted average of those states. The diffusion coefficients for the solvents ($(3.2 - 6.5) \times 10^{-10}$ m^2 s^{-1} for EMC and 5.1×10^{-10} m^2 s^{-1}) were larger than for Li$^+$ ($(2.0 - 2.8) \times 10^{-10}$ m^2 s^{-1}) and the anions ($(1.8 - 2.9) \times 10^{-10}$ m^2 s^{-1}) for all the electrolytes examined. This indicated that there were free solvent molecules and solvated solvents in those electrolytes. The diffusion coefficients for EMC in the EMC single solvent electrolytes (5.6×10^{-10} m^2 s^{-1} and 6.5×10^{-10} m^2 s^{-1}) were larger than that for the MFE/EMC mixed solvent electrolyte (3.2×10^{-10} m^2 s^{-1}). This indicated that there was less free EMC in the MFE/EMC electrolyte than in the EMC single solvent electrolytes, for the solvated solvent must show a smaller diffusion coefficient than the free solvent due to the increase of effective size. Moreover, the diffusion coefficient of EMC (3.2×10^{-10} m^2 s^{-1}) became closer to those for Li$^+$ and BETI$^-$ (1.8×10^{-10} m^2 s^{-1} and 2.0×10^{-10} m^2 s^{-1}, respectively) in MFE/EMC electrolyte. Thus, EMC must solvate more Li$^+$ strongly than MFE in 1 M LiBETI–MFE/EMC electrolyte. This agreed with the conclusion obtained from the solvation shift analysis that EMC selectively solvated Li$^+$ rather than MFE.

The conductivity σ is given by the modified Nernst–Einstein equation including the association constant of the salt [26] as presented in Equation 5:

$$\sigma = \left(\frac{1}{K_a}\right)\left(\frac{Ne^+e^-}{K_b T}\right)(D^+ + D^-) \quad (5)$$

(K_a is the association constant, N is the total number of negative and positive charges, e^+ and e^- denote the

positive and negative charges, respectively, K_b is the Boltzmann constant, T denotes the absolute temperature, and D^+ and D^- are the diffusion coefficients of Li$^+$ and anion, respectively.) By comparing experimental conductivities, we could estimate the association constant K_a. The experimental conductivity σ_{exp} and calculated K_a values are listed in Table 5. The association constant K_a for 1 M LiBETI–MFE/EMC was much larger than K_a for 1 M LiBETI–EMC and 1 M LiPF$_6$–EMC electrolytes. In this electrolyte, the ratio of EMC/lithium salt was about 2:1. Thus, there was a lack of solvent molecules to achieve a fully solvated state of Li$^+$ and anions. Consequently, the number of ion-pair states may increase to depress the conductivity of this electrolyte. Because there were few free EMC molecules in 1 M LiBETI–MFE/EMC, the diffusion constant of EMC became small, but there were many free MFE molecules, leading to a high diffusion coefficient (5.1×10^{-10} m^2 s^{-1}) in this system.

3.5. *Graphite/LiCoO$_2$ charge–discharge performances and nailing test results*

We fabricated a graphite/LiCoO$_2$ 18650 type cylindrical cell using 1 M LiBETI–MFE/EMC (80:20) electrolyte to examine charge–discharge and cycle life performances. Figure 7 shows the voltage curve during discharge at a current rate of 0.1 *C* (140 mA). The cell using 1 M LiBETI–MFE/EMC (80:20) electrolyte discharged the
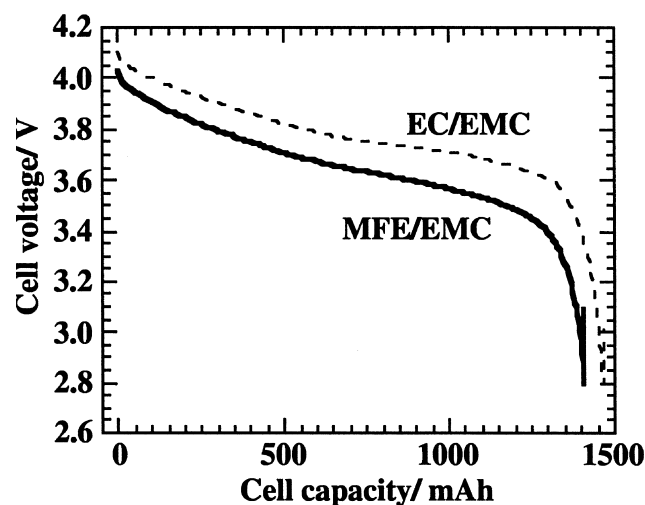

Fig. 7. Voltage profiles in the discharge of the graphite/LiCoO$_2$ 18650 cells composed of 1 M LiBETI–MFE/EMC (80:20) and 1 M LiPF$_6$–EC/EMC (30:70) at the rate of 0.1 *C* (140 mA).

same capacity as 1 M LiPF$_6$–EC/EMC(30:70) electrolyte, though there was about a 0.1 V excess voltage drop in LiBETI–MFE/EMC electrolyte compared to LiPF$_6$–EC/EMC. Very little polarization was observed during discharge in the cell using 1 M LiBETI–MFE/EMC, though the conductivity of this electrolyte (0.56 mS cm^{-1}) was about 1/16 of that of 1 M LiPF$_6$–EC/EMC (9.3 mS cm^{-1}). The possibility of nonflammable electrolyte use of MFE was demonstrated. This electrolyte is applicable to low current usage such as for load-levelling support.

Figure 8 shows the charge–discharge current rate performance of the 18650 cell using 1 M LiBETI–MFE/EMC (80:20) electrolyte. The cell was charged and discharged at currents of 0.3, 0.5 and 0.9 C (420, 700, 1260 mA, respectively). Although the high rate current increased the voltage drop, the voltage curves for all the currents were not suppressed significantly. This indicated that polarization due to the electrolyte was not significant. This is supported by the diffusion coefficients of Li$^+$ and BETI$^-$, which are similar to those observed in 1 M LiBETI–EMC. However, the rate performance of 1 M LiBETI–MFE/EMC was not sufficient for wide application. It should be improved in terms of controlling the electrode surface film condition to raise the rate of Li$^+$ exchange or modifying the lithium salt to increase its dissociation. We are studying these points to improve the cell performance.

Figure 9 shows the cycle life performance of the 18650 cell using 1 M LiBETI–MFE/EMC(80:20) and 1 M LiPF$_6$–EC/EMC(30:70) operated at 0.1 C current rate (140 mA). The 1 M LiBETI–MFE/EMC showed a fairly good cycle performance up to 30 cycles (about one month). The cell maintained 80% of the initial capacity for more than 50 cycles. The main cause of the capacity fading was the increase in cell resistance, because the discharge curve at high cycle number showed a larger voltage drop than that for the initial cycle, though more
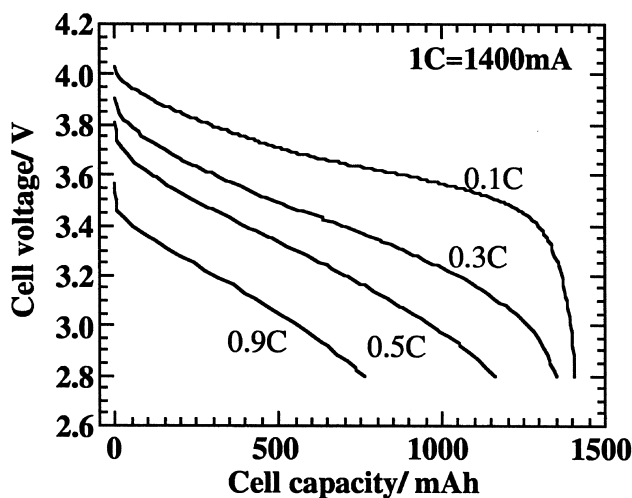

Fig. 9. Cycle life for the graphite/LiCoO$_2$ 18 650 cell composed of 1 M LiBETI–MFE/EMC (80:20) and LiPF$_6$–EC/EMC (30:70) at the rate of 0.1 C (140 mA).

analysis is needed to determine the electrochemical reactions.

An abuse test was performed to demonstrate the safety improvement which the new electrolytes give. The nailing test, in which a fully charged cell is penetrated by a nail, was selected as an abuse test, because the 18650 cells we fabricated were equipped with the CID and PTC device for overcharge protection. Before the nailing test, the cells were charged to 4.3 V (120% of charge, 20% overcharged). Figure 10 shows the nailing test results, expressed in terms of cell surface temperature during the test. The 1 M LiBETI–MFE/EMC cell was penetrated by a nail at a rate of 1 mm s^{-1}. For the 1 M LiPF$_6$–EC/EMC cell, the cell temperature rose suddenly after nail penetration due to the rapid chemical reaction which was followed by an internal short circuit. But, the 1 M LiBETI–MFE/EMC cell did not show thermal runaway and its maximum cell surface temperature was

Fig. 8. Voltage profiles in the discharge of the graphite/LiCoO$_2$ 18650 cell composed of 1 M LiBETI–MFE/EMC (80:20) at various current rates.
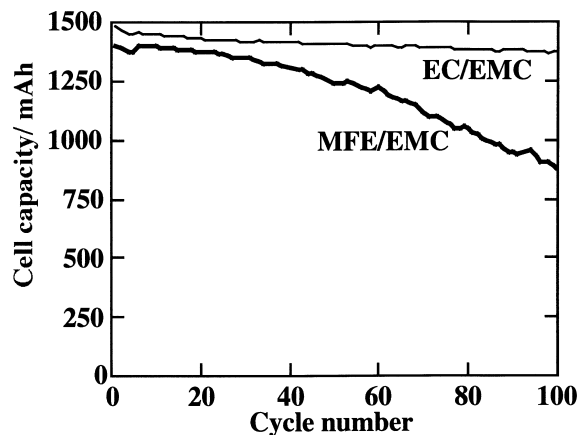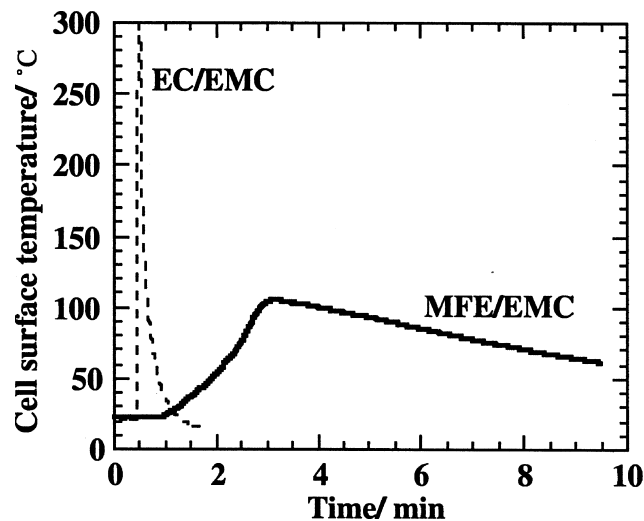

Fig. 10. The cell surface temperature of the graphite/LiCoO$_2$ 18650 cells composed of 1 M LiBETI–MFE/EMC (80:20) and 1 M LiPF$_6$–EC/EMC (30:70) in the nailing test at the nail penetration rate of 1 mm s^{-1}.

below 115 °C. No abnormalities were observed during the spontaneous cooling period. We demonstrated that the MFE not only eliminated the flash point of the electrolyte solution, but also improved the safety as seen in the abuse test.

4. Conclusions

To improve the inherent safety of lithium secondary batteries, we investigated the use of nonflammable fluorinated solvent (AFE) for the electrolyte. We found that appropriate amounts of MFE eliminated the flash point of mixed solvent solutions with common electrolyte solvents such as linear carbonates and linear ethers, though AFE was best mixed with only low dipole moment solvents. The electrolyte flash point was examined for AFE/linear carbonate and AFE/linear ether mixed solvent solutions. The MFE/EMC electrolyte was prepared by dissolving organic lithium salts such as LiTFSI, LiBETI and LiFBMSI in it, though the conductivities of the electrolytes were rather smaller than those of common electrolytes such as $LiPF_6$–EC/ EMC. Analysis using the NMR chemical shift and PFG-NMR method showed these salts were solvated dominantly by EMC in LiBETI-MFE/EMC electrolyte. We fabricated a graphite/$LiCoO_2$ 18650 cylindrical cell using 1 M LiBETI–MFE/EMC (80:20) and examined its performance, including rate capability and cycle life. An abuse (nailing) test was also carried out. We demonstrated that the 1 M LiBETI–MFE/EMC could work under low current operation for several tens of charge-discharge cycles, though the rate capability and the cycle life can be further improved. Better safety of the lithium secondary battery using 1 M LiBETI–MFE/ EMC was confirmed by the nailing test. The cell did not show thermal runaway when penetrated by a nail, even after the cell was overcharged.

Acknowledgement

References

1. M. Winter, J.O. Besenhard, M.E. Spahr and P. Novák, *Adv. Mater.* **10** (1998) 725.
2. M.C. Smart, B.V. Batnakumar, S. Surampudi, Y. Wang, X. Zhang, S.G. Greenbaum, A. Hightower, C.C. Ahn and B. Fultz, *J. Electrochem. Soc.* **146** (1999) 3963.
3. M.S. Ding, K. Xu and T.R. Jow, *J. Electrochem. Soc.* **147** (2000) 1688.
4. M. Morita, O. Yamada, M. Ishikawa and Y. Matsuda, *J. Appl. Electrochem.* **28** (1998) 209.
5. K. Hayashi, Y. Nemoto, S. Tobishima and J. Yamaki, *Electrochim. Acta* **44** (1999) 2337.
6. C.W. Lee, R. Venkatachalapathy and J. Prakash, *Electrochem. Solid-State Lett.* **3** (1999) 63.
7. D. Peramunage, J.M. Ziegelbauer and G.L. Holleck, *in* Abstracts of Fall Meeting of the Electrochemical Society, Abstract 144, Phoenix, AZ (2000).
8. K. Xu, M.S. Ding, S. Zhang, J.L. Allen and T.R. Jow, *in* Abstracts of 52nd Meeting of the International Society of Electrochemistry, Abstract 118, San Francisco (2001).
9. H. Katayama, J. Arai and H. Akahoshi, *J. Power Sources* **81–82** (1999) 705.
10. J. Arai, H. Katayama and H. Akahoshi, *J. Electrochem. Soc.* **149** (2002) A217.
11. J. Arai, K. Nishimura, Y. Muranaka and Y. Ito, *J. Power Sources* **68** (1997) 304.
12. J. Arai, H. Katayama, H. Morooka, T. Takamura, Y. Muranaka and Y. Ito, *in* C.F. Holmes and A.R. Landgrebe (Eds), 'Batteries for Portable Applications and Electric Vehicles', Electrochemical Society Proceedings B. Series, Pennington, NJ (1997), PV97–18, p. 40.
13. W.S. Price, *Concepts Magn. Reson.* **9** (1997) 299.
14. Y. Saito, H. Yamamoto, O. Nakamura, H. Kageyama, H. Ishikawa, T. Miyoshi and M. Matsuoka, *J. Power Sources* **81–82** (1999) 772.
15. K. Hayamizu, Y. Aihara, S. Arai and W.S. Price, *Solid State Ionics* **107** (1998) 1.
16. E.O. Stejskal, *J. Chem. Phys.* **43** (1965) 3597.
17. A. Webber, *J. Electrochem. Soc.* **138** (1991) 2586.
18. L. Peter and J. Arai, *J. Appl. Electrochem.* **29** (1999) 1053.
19. R.J. Blint, *J. Electrochem. Soc.* **142** (1995) 696.
20. R.J. Blint, *J. Electrochem. Soc.* **144** (1997) 787.
21. Y. Matsuda, M. Morita and T. Yamashita, *J. Electrochem. Soc.* **131** (1984) 2821.
22. H. Nakamura, H. Komatsu and M. Yoshio, *J. Power Sources* **62** (1996) 219.
23. K. Izutsu, T. Nakamura, K. Miyoshi and K. Kurita, *Electrochim. Acta* **41** (1996) 2523.
24. Y.-O. Kim and S.-M. Park, *J. Electrochem. Soc.* **148** (2001) A194.
25. A. Carrington & A.D. Mclachlan, '*Introduction to Magnetic Resonance*' (Harper & Row, New York, 1969), p. 221.
26. V.A. Payne, M. Forsyth, M.A. Ratner, D.F. Shriver and S.W. de Leeuw, *J. Chem. Phys.* **100** (1990) 5201.